Part I - Analytical Option Formulae

Our valuation approach is based on the martingale framework for option pricing, which links the current price of a contingent claim to its discounted expected payoff under the risk-neutral measure, ensuring no arbitrage. The key equation is:

$$\frac{V_0}{B_0} = \mathbb{E}^{\mathbb{Q}}\left[\frac{V_T}{B_T}\right]$$

Where, V_0 and V_T are the option's current value and payoff at maturity, while B_0 and B_T are the numéraire values (e.g., risk-free bond) at times 0 and T. Under the risk-free rate r, $B_T = B_0 e^{rT}$, simplifying the equation to:

$$V_0 = e^{-rT}\,\mathbb{E}^{\mathbb{Q}}[V_T]$$

This shows the option's value is the present value of its expected payoff under the risk-neutral measure. To value an option under this framework we first, need to define the payoff function V_T of the option at maturity, which depends on the type of option:

- Vanilla Call Option: $V_T = \max(S_T - K, 0)$
- Vanilla Put Option: $V_T = \max(K - S_T, 0)$
- Digital Cash-or-Nothing Call: $V_T = C$ if $S_T > K$, otherwise $V_T = 0$
- Digital Asset-or-Nothing Call: $V_T = S_T$ if $S_T > K$, otherwise $V_T = 0$

Here, S_T is the underlying asset price at maturity, K is the strike price, and C is a fixed cash amount for the digital option. We model the dynamics of the underlying asset price S_t using the following stochastic processes:

- Black Model: $dF_t = \sigma F_t\, dW_t$
- Black-Scholes: Geometric Brownian motion: $dS_t = \mu S_t dt + \sigma S_t dW_t$
- Bachelier: Arithmetic Brownian motion: $dS_t = \mu dt + \sigma dW_t$
- Displaced-Diffusion: Dynamics adjusted by a displacement factor β:

$$dS_t = \mu(S_t + \beta)dt + \sigma(S_t + \beta)dW_t$$

Note that, μ is the drift, σ the volatility, and dW_t the increment of a Wiener process.Under the risk-neutral measure $\mathbb{Q}$, μ is adjusted to represent the risk-free rate r. Intuitively, this reflects the market maker's view of being indifferent to directional exposure, leaving only the risk-free return. Mathematically, this adjustment is made by changing the measure using the Radon-Nikodym derivative and Girsanov's theorem, ensuring the expected return equals r to eliminate arbitrage. To determine the option's current value V_0, we begin by identifying the region where the payoff V_T is non-zero and adjust the integration bounds accordingly. This ensures the integral reflects the specific payoff structure. We then express V_0 as the discounted expected payoff under the risk-neutral measure:

$$V_0 = e^{-rT}\,\mathbb{E}^{\mathbb{Q}}[V_T] = e^{-rT}\int_a^b V_T\, f_{S_T}(s)\, ds$$

Here, $[a, b]$ represents the adjusted integration bounds where $V_T > 0$, and $f_{S_T}(s)$ is the probability density function of the underlying price S_T at maturity under the risk-neutral measure. Following this core approach, we have derived the payoffs mentioned earlier under the specified models. The final analytical solutions are presented in Table 1, with detailed derivation steps available in the accompanying Python script `part1.py`.

Part II - Model Calibration

On December 1st, 2020, the S&P500 (SPX) index stood at 3662.45, and the SPDR S&P500 ETF (SPY) was priced at 366.02. Using provided datasets, including SPX options, SPY options, and the discount rate from zero rates as of December 1st, we extracted the market implied volatility using Black-Scholes and subsequently calibrated the Displaced-Diffusion and SABR models to fit the observed option prices and generated the implied volatility smiles. This section walks through the calibration process, fitted results, and how different model parameters influence the volatility smile.

Model	Vanilla call/put	Digital cash-or-nothing call/put	Digital asset-or-nothing call/put
Black-Scholes	$d_1 = \frac{\log \frac{S_0}{K} + \left(r + \frac{\sigma^2}{2}\right)T}{\sigma\sqrt{T}}$ $d_2 = d_1 - \sigma\sqrt{T}$ $C_{BS,v} = S_0\Phi(d_1) - Ke^{-rT}\Phi(d_2)$ $P_{BS,v} = Ke^{-rT}\Phi(-d_2) - S_0\Phi(-d_1)$	$C_{BS,c} = e^{-rT}\Phi(d_2)$ $P_{BS,c} = e^{-rT}\Phi(-d_2)$	$C_{BS,a} = S_0\Phi(d_1)$ $P_{BS,a} = S_0\Phi(-d_1)$
Bachelier	$d = \frac{S_0 - K}{\sigma\sqrt{T}}$ $C_{Ba,v} = e^{-rT}\left[(S_0 - K)\Phi(d) + \sigma\sqrt{T}\phi(d)\right]$ $P_{Ba,v} = e^{-rT}\left[(K - S_0)\Phi(-d) + \sigma\sqrt{T}\phi(-d)\right]$	$C_{Ba,c} = e^{-rT}\Phi(d)$ $P_{Ba,c} = e^{-rT}\Phi(-d)$	$C_{Ba,a} = S_0\Phi(d) + \sigma\sqrt{T}\phi(d)$ $P_{Ba,a} = S_0\Phi(-d) + \sigma\sqrt{T}\phi(-d)$
Black	$d_1 = \frac{\log \frac{F_0}{K} + \frac{\sigma^2}{2}T}{\sigma\sqrt{T}}$ $d_2 = d_1 - \sigma\sqrt{T}$ $C_{B,v} = e^{-rT}\left[F_0\Phi(d_1) - K\Phi(d_2)\right]$ $P_{B,v} = e^{-rT}\left[K\Phi(-d_2) - F_0\Phi(-d_1)\right]$	$C_{B,c} = e^{-rT}\Phi(d_2)$ $P_{B,c} = e^{-rT}\Phi(-d_2)$	$C_{B,a} = F_0e^{-rT}\Phi(d_1)$ $P_{B,a} = F_0e^{-rT}\Phi(-d_1)$
Displaced-diffusion	$d_1 = \frac{\log \frac{F_0 + \beta(K - F_0)}{\beta} + \frac{\sigma_\beta^2}{2}T}{\sigma_\beta\sqrt{T}}$ $d_2 = d_1 - \sigma_\beta\sqrt{T}$ $C_{D,v} = C_{B,v}\left(\frac{F_0}{\beta}, K + \frac{1-\beta}{\beta}F_0, r, \beta\sigma, T\right)$ $P_{D,v} = P_{B,v}\left(\frac{F_0}{\beta}, K + \frac{1-\beta}{\beta}F_0, r, \beta\sigma, T\right)$	$C_{D,c} = e^{-rT}\Phi(d_2)$ $P_{D,c} = e^{-rT}\Phi(-d_2)$	$C_{D,a} = \frac{F_0}{\beta}\Phi(d_1)$ $P_{D,a} = \frac{F_0}{\beta}\Phi(-d_1)$

Table 1: Comparison of pricing models for vanilla and digital options.

Market Implied Volatility

When it comes to options in any asset class, an important phenomenon is how option prices vary with respect to time to maturity and strike prices. Combined, these dimensions form a three-dimensional figure known as the volatility surface. From this surface, two additional popular visualization methods emerge. One is the term structure of volatility, which fixes options at a certain strike and examines how volatility evolves across different maturities. The other is fixing the time to maturity and observing how volatility changes with strike prices, resulting in the implied volatility smile or skew. In FX markets, a symmetric volatility smile is often expected due to the balanced nature of exchange rates. However, in equity markets, the smile is typically asymmetric around the ATM point, earning it the term 'skew' or 'smirk' in practice. Since we are focusing on equity index options in this project, we will examine the economic intuition behind this observed skew in implied volatility. There is a negative correlation between equity prices and volatility. As prices move down, volatilities tend to move up, and vice versa. One reason for this is leverage: as equity prices decline, leverage increases, leading to higher volatility. Another factor is the volatility feedback effect, where increased volatility prompts investors to demand a higher return, resulting in lower stock prices. Additionally, 'crashophobia,' or fear of sudden market drops, contributes to the asymmetry. Consequently, declines in stock prices are often accompanied by increased volatility, amplifying the likelihood of further drops. On the other hand, price increases lead to reduced volatility. The volatility smile for equity options also suggests that the implied distribution has a heavier left tail and a less heavy right tail compared to the lognormal distribution.[1]

Displaced-Diffusion Model

The Displaced-Diffusion model is a straightforward extension of the Black-Scholes model that introduces a displacement parameter to capture the skewness observed in real-world markets. This adjustment effectively shifts the underlying asset price, providing better control over how volatility behaves concerning moneyness—the relationship between the strike price and the current price of the underlying asset. The key parameters in the Displaced-Diffusion model are:

- σ (sigma): The volatility of the underlying asset.
- β (beta): The displacement factor, allowing the model to capture shifts in implied volatility patterns.

In this model, the displacement factor $\beta \in [0, 1]$ plays a significant role in modifying the dynamics of the underlying asset's price S_0. Specifically, β controls the degree to which S_0 influences the asset's volatility:

[1] John C. Hull, *Options, Futures, and Other Derivatives*, 10th edition, Pearson, 2018.

- When $\beta = 1$: The model reduces to the standard Black-Scholes model, where the volatility term is simply σS_0. This means the volatility is directly proportional to the asset's price.
- When $\beta = 0$: The model's dynamics are dominated by a constant F_0, making the volatility independent of the asset's price. In this case, the volatility term becomes σF_0.
- When $0 < \beta < 1$: The model incorporates a blend of both the asset's price S_0 and the constant F_0. This allows the model to capture scenarios where the volatility is not entirely proportional to the asset's price but is also influenced by some baseline level represented by F_0.

In general, a higher β implies that the volatility is more strongly tied to the asset's price, while a lower β suggests that the volatility is more dependent on the constant F_0. This flexibility makes the Displaced-Diffusion model useful for modeling situations where the asset's price volatility does not behave purely as a linear function of its current price. By adjusting β, the Displaced-Diffusion model can capture the observed skewness in implied volatility surfaces, which the standard Black-Scholes model cannot adequately address due to its assumption of constant volatility. The displacement parameter allows the model to better fit market data by adjusting the relationship between the asset price and volatility, providing a more accurate representation of option prices across different strikes.

SABR Model

The SABR model is a well-known stochastic volatility model used to approximate the implied volatility of options. The implied volatility for a European option with strike price K is given by the formula:

$$\begin{cases} dF_t = \alpha_t F_t^{\beta} dW_t^F, \\ d\alpha_t = \nu \alpha_t dW_t^{\alpha}, \end{cases} \qquad \text{where} \quad dW_t^F \, dW_t^{\alpha} = \rho \, dt.$$

$$\begin{aligned} \sigma_{\text{SABR}}(F_0, K, \alpha, \beta, \rho, \nu) = {} & \frac{\alpha}{(F_0 K)^{(1-\beta)/2}} \left\{ 1 + \frac{(1-\beta)^2}{24} \log^2 \left(\frac{F_0}{K} \right) + \frac{(1-\beta)^4}{1920} \log^4 \left(\frac{F_0}{K} \right) + \dots \right\} \\ & \times \frac{z}{x(z)} \\ & \times \left\{ 1 + \left[\frac{(1-\beta)^2}{24} \frac{\alpha^2}{(F_0 K)^{1-\beta}} + \frac{1}{4} \frac{\rho \beta \nu \alpha}{(F_0 K)^{(1-\beta)/2}} + \frac{2 - 3\rho^2}{24} \nu^2 \right] T + \dots \right\}, \end{aligned}$$

$$z = \frac{\nu}{\alpha} (F_0 K)^{(1-\beta)/2} \log \left(\frac{F_0}{K} \right), \quad \text{and} \quad x(z) = \log \left[\frac{\sqrt{1 - 2\rho z + z^2} + z - \rho}{1 - \rho} \right].$$

In the SABR (Stochastic Alpha Beta Rho) model, the parameter **Alpha** (α) adjusts the height of the implied volatility curve and serves as the initial volatility level. It acts as a baseline implied volatility (IV) that influences all option prices across different strikes. Unlike the deterministic volatility assumed in the Black-Scholes model, the SABR model introduces stochastic volatility that can be correlated with the underlying asset's returns. The parameter **Rho** (ρ) represents this correlation between the asset price and its volatility. Specifically, ρ adjusts for the skewness in the distribution of stock returns. A negative value of ρ introduces a negative skew, implying that volatility tends to increase when stock prices decrease. This adjustment raises the implied volatilities of lower-strike options (out-of-the-money puts) and lowers the implied volatilities of higher-strike options (out-of-the-money calls), providing a better fit to observed market prices than the Black-Scholes model. This negative correlation also reflects behavioral factors: investors are typically more concerned about downside risks than upside potentials. Consequently, they are willing to pay higher premiums for protective OTM puts compared to equally distant OTM calls, leading to higher implied volatilities for lower strikes. The parameter **Nu** (ν) adjusts for the volatility of volatility and is related to the kurtosis (fat tails) of the returns distribution. A higher value of ν increases the curvature of the implied volatility smile, elevating the implied volatilities (and thus the prices) of both calls and puts relative to at-the-money options. When combined with a negative ρ, this results in an implied volatility curve that more accurately fits market prices and captures both the skewness and kurtosis observed in real-world data. In contrast, the **Displaced-Diffusion model** lacks sufficient degrees of freedom to effectively fit market implied volatilities. It cannot capture the skewness and kurtosis observed in actual option price data due to its more restrictive structure. The SABR model, however, is capable of fitting the implied volatility surface well and is popular due to its computational efficiency. Specifically, it provides analytical approximations for implied volatility, which allows for quick calculations without the need

for numerically solving complex stochastic differential equations. This makes the SABR model both practical and effective for modeling implied volatility surfaces in financial markets. The SABR model offers a robust framework for capturing the complexities of the implied volatility surface by incorporating stochastic volatility and accounting for skewness and kurtosis in asset returns. Its parameters—α, ρ, and ν—provide the necessary flexibility to align closely with market data, addressing the limitations of simpler models like Black-Scholes and Displaced-Diffusion. Additionally, the SABR model's analytical approximations enhance its practicality, making it a preferred choice for practitioners in the field of option pricing.

Compute Market IV

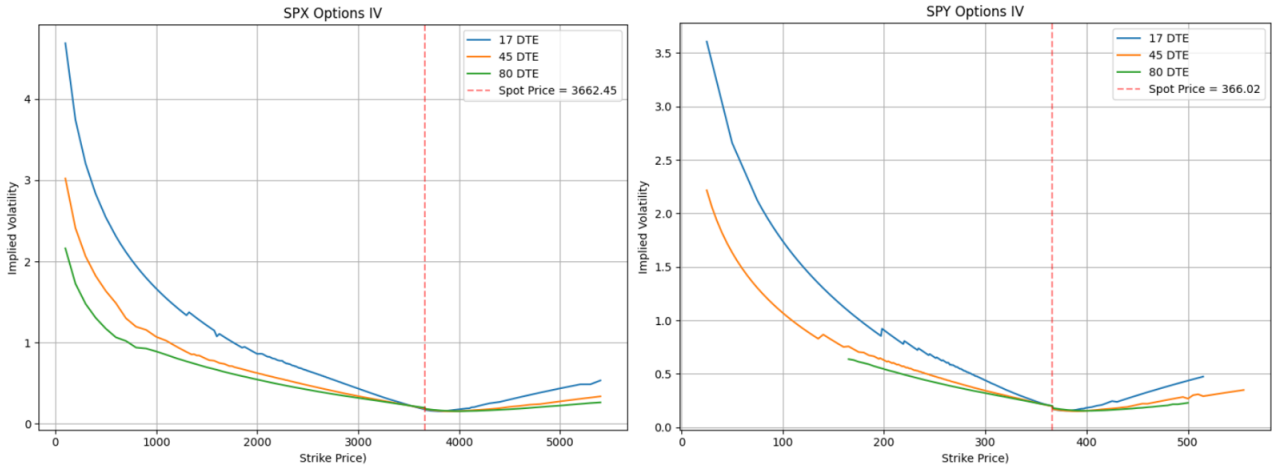

Figure 1: Visualization of market Implied Volatility

The IV for SPX is higher than SPY's due to differences in contract structure. SPX options are cash-settled (European-style) with a multiplier of 100, attracting institutional investors. SPY options are physically settled (American-style) with a multiplier of 1, suiting retail traders. IV also varies with expiration: near-term options (e.g., 17 DTE) have higher IV due to their gamma sensitivity, reflecting short-term uncertainty, while longer-term options (e.g., 80 DTE) smooth out volatility. At the money (ATM), IV converges across expirations, as explained by the Black-Scholes model: At $S_0 = K$, these simplify to:

$$d_1 \approx \frac{\left(r + \frac{\sigma^2}{2}\right) T}{\sigma\sqrt{T}}, \quad d_2 \approx -\frac{\sigma\sqrt{T}}{2}.$$

This shows that ATM options' sensitivity to strike price and DTE diminishes, leading to similar IV behavior across expirations.

Displaced Diffusion Model Calibration

Moving on, we are going to calibrate the DD model to suit the market IV. In this section, we calibrate the model by parsing the calculated market IV, spot price, and risk-free rates. This calibration minimizes the least squared error between market IV and model IV, as well as the displacement parameter $\beta \in [0, 1]$, using the following formula:

$$\min_{\beta,\sigma} \sum_{i=1}^{N} \left(IV_{\text{market},i} - IV_{\text{model},i}(\beta, \sigma)\right)^2$$

As a result, we obtain the table of calibrated parameters for different tickers with respect to different Days-to-Expiry (DTE):

SABR Model Calibration

The goal here is similar to the DD model calibration, but we have different parameters to calibrate. As we know, SABR stands for Stochastic Alpha Beta Rho, and we need to calibrate the parameters for Alpha (α),

DTE	Sigma (SPX)	Beta (SPX)	Sigma (SPY)	Beta (SPY)
17	0.174485	4.19E-07	0.200906	1.30E-07
45	0.184910	1.92E-11	0.197218	1.13E-06
80	0.193747	4.22E-07	0.200240	1.14E-05

Table 2: Displaced Diffusion Calibrated Parameters

Beta (β), Rho (ρ), and Nu (ν). Here, we implement the same logic to minimize the squared error between the market IV and the SABR model IV by adjusting these parameters. The error is calculated as:

$$\text{Error} = \sum_{i=1}^{N} \left(IV_{\text{market},i} - IV_{\text{SABR},i}(\alpha, \beta, \rho, \nu)\right)^2$$

DTE	F (SPX)	α (SPX)	ρ (SPX)	ν (SPX)	β (SPX)
17	3662.664	1.2123	-0.3009	5.4598	0.7
45	3663.376	1.8165	-0.4043	2.7902	0.7
80	3664.221	2.1401	-0.5749	1.8417	0.7

Table 3: SABR Calibrated Parameters for SPX

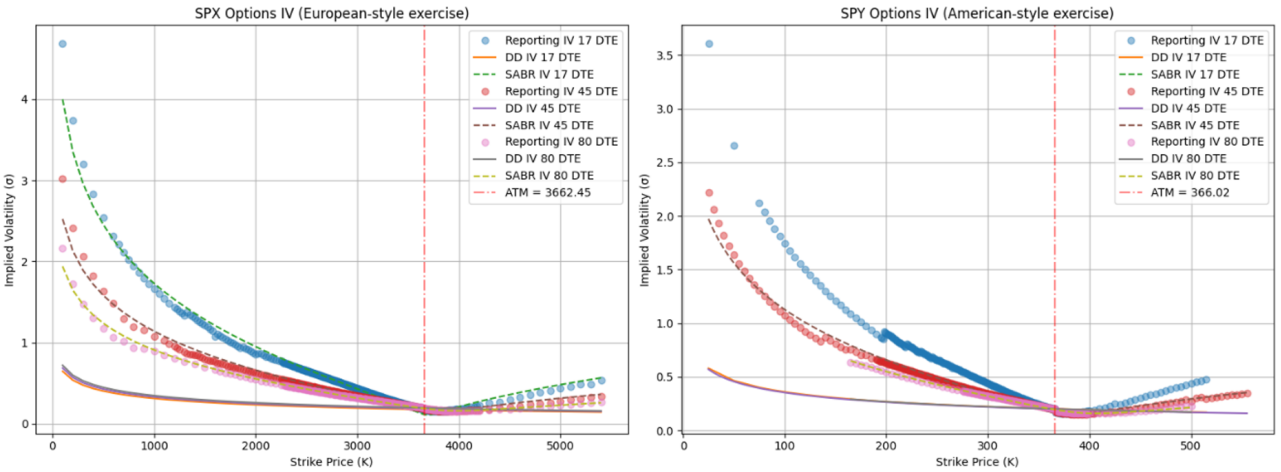

Figure 2: Visualization of SABR, DD and MKT IV

From the results, we can see that the DD model's IVs are accurate only when the strike price is close to the spot price. This limitation arises because the DD model lacks sufficient degrees of freedom to closely fit market-implied volatilities. Specifically, in the presence of volatility skew, far out-of-the-money (OTM) or deep in-the-money (ITM) options often exhibit pronounced skew effects, which the DD model struggles to replicate accurately. In contrast, the SABR model is explicitly designed to capture both skew and smile effects. The beta parameter acts as an elasticity control, determining the degree of non-linearity in the forward price processes. Additionally, the rho parameter and the volatility of volatility introduce stochastic dynamics and skew effects, enabling the SABR model to closely match market IVs across a wider range of strikes, including deep OTM and deep ITM options.

Part III - Static Replication

In this section, we investigate the valuation of exotic derivatives under two different frameworks.

Non-Standard Payoff Structure

We examine an exotic derivative with a non-standard payoff structure, observed on December 1, 2020, with maturity on January 15, 2021. The derivative's payoff at maturity is defined as:

$$h(S_T) = S_T^{1/3} + 1.5\ln(S_T) + 10.0$$

where S_T represents the underlying asset price at maturity. This payoff function combines two concave terms ($S_T^{1/3}$ and $\ln(S_T)$) with diminishing marginal returns, resulting in a monotonically increasing function. The cube root term ($S_T^{1/3}$) provides exposure to upward price movements while dampening extreme outcomes. The logarithmic component ($1.5\ln(S_T)$) adds further convexity to the payoff, and the constant term (10.0) shifts the payoff and establishes a baseline level. We will revisit these properties in later parts of the discussion.

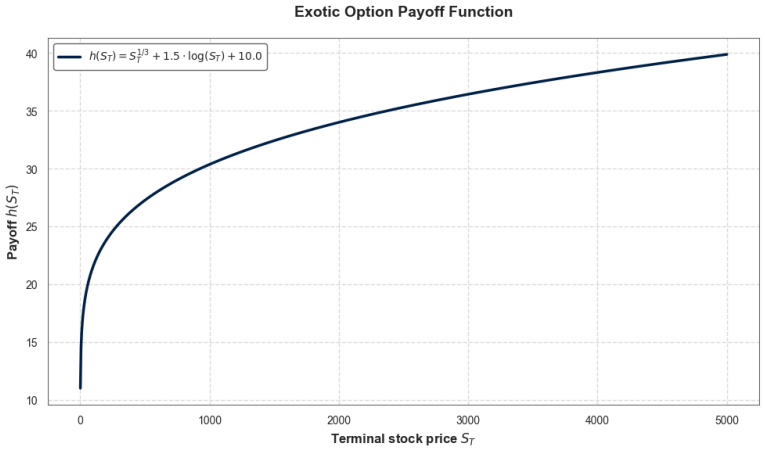

Figure 3: Visualization of the exotic payoff function $h(S_T)$

Model-Free Variance Framework

The second framework we consider involves the model-free variance, defined as:

$$\sigma_{\text{MF}}^2 T = \mathbb{E}\left[\int_0^T \sigma_t^2 \, dt\right],$$

where σ_t^2 represents the instantaneous variance of the underlying asset, and T is the time to maturity. The model-free integrated variance, denoted as $\sigma_{\text{MF}}^2 T$, represents the expected value of the integral of the instantaneous variance of the underlying asset's returns over the time horizon $[0, T]$. It is a forward-looking measure of the total variance accumulated by the underlying asset's price over a given time frame.

Determining the Price of the Contracts

To evaluate these contracts under the Bachelier and Black-Scholes models both of which assume constant arithmetic and geometric variance, respectively, we calculate an arithmetic average over different strikes. For both models, we compute:

$$\sigma_{\text{model}}^2 = \left(\frac{1}{N}\sum_{i=1}^{N} \sigma(K_i)\right)^2,$$

where $\sigma(K_i)$ represents the implied volatility (Bachelier or Black-Scholes, respectively) from puts when $S_0 > K_i$ and calls when $S_0 < K_i$ across N different strikes. In the case of the Bachelier model, we interpret volatilities in terms of absolute price changes, while in the Black-Scholes model, we interpret them as percentage changes. Under static replication, we follow a different approach to evaluate the payoff, using:

$$V_0 = e^{-rT}h(F) + \underbrace{\int_0^F h''(K)P(K)\,dK}_{\text{put integral}} + \underbrace{\int_F^\infty h''(K)C(K)\,dK}_{\text{call integral}},$$

where $h''(K)$ is the second derivative of the payoff function with respect to the strike price K, given by:

$$h''(S_T) = -\frac{2}{9}S_T^{-5/3} - \frac{1.5}{S_T^2}.$$

For the "model-free" integrated variance equation under static replication, we use:

$$T = \mathbb{E}\left[\int_0^T \sigma_t^2\, dt\right] = 2e^{rT}\left(\int_0^F \frac{P(K)}{K^2}\, dK + \int_F^\infty \frac{C(K)}{K^2}\, dK\right).$$

To obtain a solution We perform the numerical integration using the Gaussian quadrature rule. Combining all models, we obtain the following results:

Metric	**SPX (Black-Scholes)**	**SPY (Black-Scholes)**	**SPX (Bachelier)**	**SPY (Bachelier)**	**SPX (SABR)**	**SPY (SABR)**
V_0	37.670	25.963	37.703	25.978	37.700	25.993
M	0.018	0.025	0.005	0.015	0.006	0.006
σ^2_{MF}	0.149	0.201	0.042	0.123	0.051	0.049
σ	0.386	0.448	0.205	0.350	0.227	0.221

Table 4: Metrics Comparison Across Models and Assets

Discussion

Analysing two distinct derivative contracts, an exotic payoff and a variance swap, our results reveal significant differences in their pricing sensitivities and optimal valuation approaches. These findings underscore the importance of selecting appropriate pricing methodologies based on the unique characteristics of each contract. The exotic payoff contract, defined as $S_T^{1/3} + 1.5\log(S_T) + 10.0$, exhibits favorable mathematical properties. The combination of cube root and logarithmic functions creates a very smooth payoff profile over price ranges that are typical for SPY and SPX options. Consequently, while Black-Scholes with delta hedging may suffice for the exotic payoff, the variance contract demands a more nuanced approach due to its direct exposure to volatility dynamics. The variance contract's appeal lies in its ability to capture realized variance, which can be replicated through a specific portfolio of options weighted by $\frac{1}{K^2}$. This model-free replication approach eliminates the need for restrictive assumptions about constant volatility that both Black-Scholes and Bachelier models impose. Instead, it allows market prices to directly inform our understanding of expected future variance. This distinction becomes evident through our sensitivity analysis, which reveals differences in how the two contracts respond to changes in SABR model parameters. The variance contract shows strong sensitivity to parameter adjustments, particularly to the beta (β) parameter, which controls how volatility scales with the price level. A 5% change in beta leads to a 20% change in the contract's value, highlighting the critical importance of accurate parameter specification for variance pricing. The sensitivity analysis provides several key insights into model risk and parameter importance:

- For the variance contract, our results strongly support the use of model-free approaches over traditional constant volatility assumptions. The pronounced parameter sensitivities, especially to beta, demonstrate why simplified models like Black-Scholes, which assume constant volatility, may be inadequate for variance pricing. The model-free approach, by incorporating market prices across a range of strikes, better captures the dynamic and stochastic nature of real-world volatility.
- For the exotic payoff, we observe relatively small sensitivities (around ± 0.00015 relative change), confirming its well-behaved nature. However, even in this case, beta remains the most influential parameter, albeit with a negative slope due to the concave nature of the payoff function.

Our findings emphasize that while simpler models may suffice for hedging or pricing well-behaved exotic payoffs, more sophisticated, model-independent approaches are necessary for accurately pricing contracts with direct exposure to volatility, such as variance contracts. The choice of pricing methodology should therefore be carefully considered, taking into account the specific sensitivities and characteristics of the derivative in question.

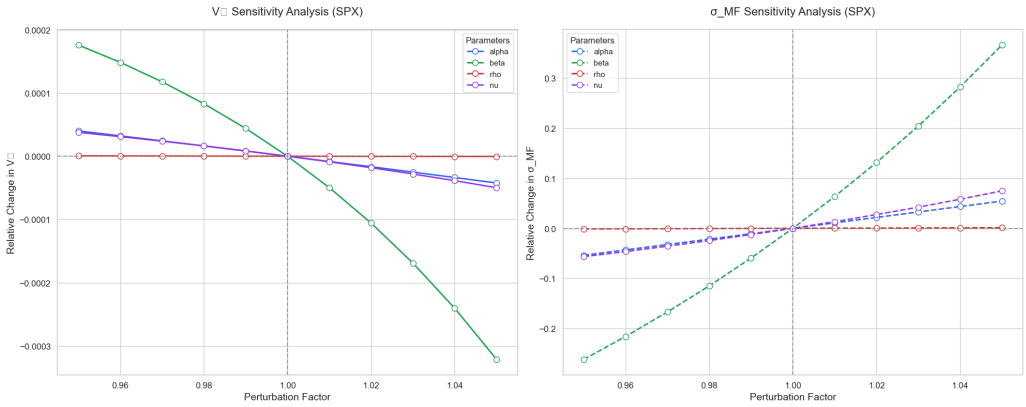

(a) Sensitivity of V_0 (Price)

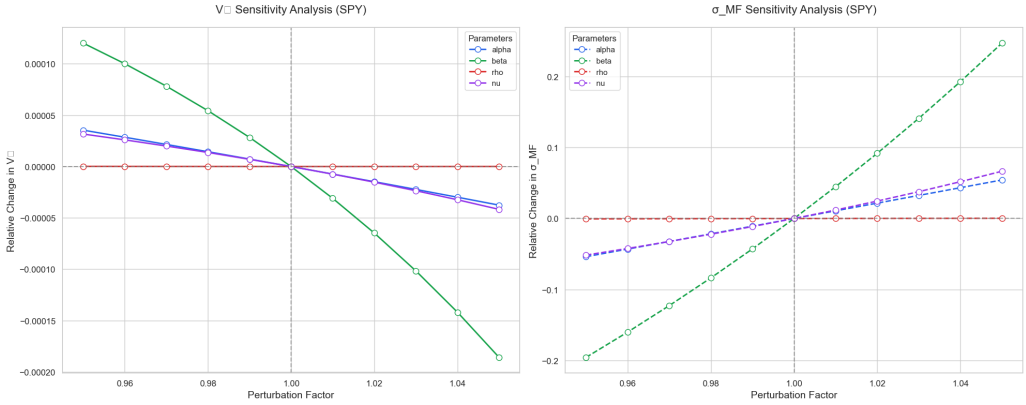

(b) Sensitivity of σ_{MF} (Implied Volatility)

Figure 4: Sensitivity Analysis of the Derivative's Price and Implied Volatility

Part IV - Dynamic Hedging

To investigate the hedging error of the dynamic delta hedging strategy when hedging dynamically, we proceed as follows. Our starting point is a European call option with parameters $S_0 = 100$, $\sigma = 0.2$, $r = 5\%$, $T = \frac{1}{12}$ year (1 month), and $K = 100$. The dynamic hedging strategy follows:

$$C_t = \phi_t S_t - \psi_t B_t,$$

where ϕ_t represents the option's delta:

$$\phi_t = \frac{\partial C}{\partial S} = \Phi\left(\frac{\ln(S_t/K) + \left(r + \frac{1}{2}\sigma^2\right)(T-t)}{\sigma\sqrt{T-t}}\right),$$

and $\psi_t B_t$ is:

$$\psi_t B_t = -Ke^{-r(T-t)}\Phi\left(\frac{\ln(S_t/K) + \left(r - \frac{1}{2}\sigma^2\right)(T-t)}{\sigma\sqrt{T-t}}\right).$$

We analyze this strategy by comparing the replicated position with the final call option payoff at maturity, implementing the hedging with $N = 21$ and $N = 84$ rebalancing timestamps across 21 days.

Analysis of Simulation Results

Our simulation results closely mirror the theoretical predictions from discrete-time hedging theory. The histograms of hedging errors for both $N = 21$ and $N = 84$ rebalancing frequencies exhibit several key characteristics:

- **Daily Rebalancing ($N = 21$):** We observe a mean hedging error of 0.01 (effectively zero) with a standard deviation of 0.43, representing approximately 17% of the option premium.

– **Four Times Daily Rebalancing ($N = 84$):** The mean remains at zero while the standard deviation decreases to 0.22, or about 9% of the premium.

This reduction in standard deviation by roughly half when quadrupling the hedging frequency aligns remarkably well with the theoretical prediction of a $1/\sqrt{N}$ relationship. The distributions in both cases are approximately normal, suggesting that the hedging error can be effectively characterized using standard statistical measures. This normality is not coincidental but rather a consequence of the central limit theorem applied to the accumulated hedging errors over multiple rebalancing periods. A critical observation is that discrete hedging introduces unavoidable errors but does not create systematic bias; the mean error remains effectively zero in both cases. This confirms that while perfect replication is impossible with discrete hedging, the Black-Scholes price remains "fair" in the sense that neither the hedger nor the option buyer has a systematic advantage. The hedging error decrease from $N = 21$ to $N = 84$ can be understood intuitively through the lens of volatility sampling: more frequent rebalancing allows for better tracking of the underlying's price movements, reducing the magnitude of individual hedging errors. However, the law of diminishing returns applies—quadrupling the hedging frequency only halves the standard deviation of errors, suggesting practical limits to the benefits of increasing hedging frequency. [2]

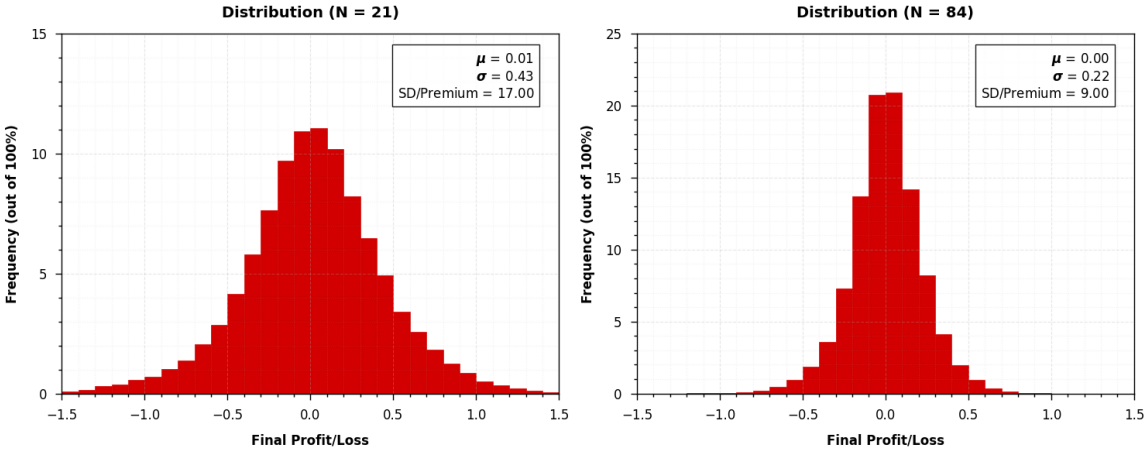

Figure 5: Hedging Error Histogram

[2] Michael Kamal, *When You Cannot Hedge Continuously: The Corrections to Black-Scholes*, Goldman Sachs Equity Derivatives Research, 1998.